Publication status: This preprint has been published elsewhere.
DOI of the published preprint: https://doi.org/10.1590/2675-2824073.25025

Microplastic Hotspots on a Tropical Estuarine-Bay System

Arian Dialectaquiz, Danilo Augusto Silva, Dalton Sasaki, Marcelo Dottori

https://doi.org/10.1590/SciELOPreprints.12903

Submitted on: 2025-08-06
Posted on: 2025-08-06 (version 1)
(YYYY-MM-DD)

Ocean and Coastal Research

http://doi.org/10.1590/2675-2824073.25025

Microplastic Hotspots on a Tropical Estuarine-Bay System

Arian Dialectaquiz [1], Danilo A. Silva [1] *, Dalton K. Sasaki [2] and Marcelo Dottori [1]
orcid.org/0000-0002-7746-8205 orcid.org/0000-0002-9714-4937 orcid.org/0000-0002-8006-0200 orcid.org/0000-0003-2382-4136

[1]Insituto Oceanográfico, Universidade de São Paulo, São Paulo, Brazil, 05508-120,
[2] Northeastern University: Nahant, MA, US , 01908
*Corresponding author: arian.santos@usp.br

Abstract

The accumulation and export of microplastics are associated with growing negative socio-environmental impacts, which are intensified in coastal and estuarine areas. The Santos Estuarine System is the most populous estuarine region and the largest seaport in Brazil, where the movement and accumulation of microplastics is an integrated effect of diverse hydrodynamic conditions. To identify the vulnerability of pollution by microplastics in extreme conditions of sea surface elevation in this complex estuarine region, the coupling between Lagrangian and Eulerian modelling was employed, an approach that has become popular in the study of ocean movements. The trajectories of microplastics from potential sources were modelled using Opendrift, forced by currents from the Eulerian model Estuarine, Coastal and Ocean Model (ECOM), and waves from Wavewatch III. Particle concentrations and three-dimensional stochastic probability of contact with the continent were evaluated, demonstrating that, regardless of the sea surface elevation condition, microplastics are more exported to the South Brazilian Bight than accumulated on the margins and/or bottom of the system. During higher elevations of the sea surface, there is a greater accumulation of microplastics on the estuary margins, with spring tide promoting faster accumulation. Although the entire coastline of Santos and adjacent beaches are prone to the largest accumulations, portions further to the Northeast of the estuary have not shown the propensity to be contaminated with microplastics released into estuarine channels. The highest concentrations are actively drifting in the system's water column.

Keywords: Lagrangian drift, ocean modelling, plastic pollution, Opendrift

INTRODUCTION

Marine pollution is the first of the challenges of the United Nations Oceans Decade, being relevant to understanding and mapping sources of pollutants and contaminants released into the sea, in addition to their potential impacts on human health and marine ecosystems (MacLeod et al. 2021). The accumulation of microplastics – due to widespread use for its production and logistics characteristics (Lebreton et al. 2017, Sterl et al. 2020) – is notoriously a form of growing pollution, having already been detected in all marine environments (Van Sebille et al. 2012). Plastic degradation occurs due to environmental conditions, leading to plastic pollution from macro to microscale (< 5 mm) (Poulain et al. 2018). Plastic particles on such a scale affect the biosphere metabolically and structurally (Kershaw et al. 2019), as well as ecologically, encompassing impacts on food webs and changes in biogeochemical cycles (Egger et al. 2020, Malli et al. 2022).

The coastal region is where the initial phase of

the processes of variations in the size and properties of plastic debris takes place, due to the high energy of the coastal and estuarine systems combined with the presence of abrasive elements (Kershaw et al. 2019, Hardesty et al. 2017). However, the use of numerical models to track and predict these particles is more often with low spatial resolutions (> 1/12º) to the open ocean (Krelling et al. 2017, Kaandorp et al. 2023).

The Santos Estuarine System (SES) (24ºS, 46.3ºW), on the South Brazil Bight (SBB), is an important study area, covering 30 km in an east-west direction and 19 km in a north-south direction (Marengo et al. 2017). Due to its interconnected estuarine channels, it has two connections with the ocean and houses the largest maritime port in Brazil (Porto de Santos) (Costa et al. 2020).

In an estuarine system such as Santos, the main factors controlling plastic drift can be summarised in the tide, abundance of microplastics, rainfall, wind, Stokes drift, and buoyancy. The effect of the ebb tide is to transport particles from the estuary to the ocean, and in flood tide to reintroduce such particles (Malli et al. 2022). Furthermore, the abundance of microplastics is higher in the estuary beds during the neap tide, and in the water column during spring tide (Gorman et al. 2020).

The increase in flow associated with rainfall is capable of resuspending microplastics in the water column (Piehl et al. 2020), and remobilising particles trapped in vegetation cover (Pinheiro et al. 2021). Concomitantly, the wind affects the suspension and deposition of microplastics (Strand et al. 2021), being able to import or export low-density films and microplastics to the estuary. Furthermore, microplastics are redistributed in the water column due to turbulent mixing caused by wind. Wind also causes Stokes drift - due to the displacing of the particle from its final position after a wave period (Dagestad & Röhrs 2019).

An anomalous situation of meteo-oceanographic conditions in a coastal and estuarine system, with great economic and environmental impact, are the storm surges - a constructive sign of the astronomical and meteorological tide with the influence of the local geomorphology (Costa et al. 2020). Storm surges influence the dispersion and accumulation of pollution in the coastal zone (Seiler et al. 2020). Such a direct influence of sea surface elevation on the transport of pollutants becomes more prominent in matters of climate change, and the consequent increase in the frequency of cold fronts, storm surges, as well as the epitome of the general rise in mean sea level (Goldenberg et al. 2001).

Several coastal-scale studies have investigated the transport and accumulation of plastic debris in Brazil. In the Paranaguá estuary, research has tracked the movement of plastic waste (Krelling et al. 2017). In the Santos estuary, seasonal variability in microplastic accumulation has been analysed, highlighting differences between wet and dry periods (Gorman et al. 2020, Balthazar-Silva et al. 2020). Additionally, a method for predicting plastic contributions using remote sensing has been proposed (da Silva Ferreira et al. 2021).

A key approach for studying pollutant dispersion is Lagrangian drift simulation, which enables rapid analysis under various physicochemical conditions (Sterl et al. 2020). However, despite its advantages, this method still presents challenges in accurately identifying when and where pollutants enter and leave different oceanic systems.

In the Santos Estuarine System (SES), sea surface elevation plays a crucial role in debris accumulation near the estuary and along the sandy beaches of Santos Bay (da Silva Ferreira et al. 2021). Additionally, wind-driven current inversions, particularly those associated with the passage of cold fronts from the southwest, further influence plastic transport patterns (Costa et al. 2020). To better understand these processes, this study integrates three numerical models: an Eulerian model for large-scale circulation, a Lagrangian model for particle tracking, and a spectral model for surface wave dynamics.

Thus, to evaluate the transport and accumulation of microplastics in the SES under the influence of different sea surface elevation conditions, this study tested the hypothesis that (i) the dynamics of the SES export microplastics to SBB under normal and extreme conditions (positive and negative) of elevation of the sea surface, and that (ii) under conditions of extreme elevation (lowering) of the sea surface, the system acts to retain a greater (lesser) amount of microplastics. By coupling Lagrangian, Eulerian, and wave models, we sought to identify the hotspots

of microplastic accumulation in Santos Bay and to quantify the annual export of microplastics from the SES to the SBB.

METHODS

Study Area

The SES is located in the central and widest part of the South Brazil Bight (SBB), and is classified as partially mixed (Hansen & Rattray 1962). The SES is under the influence of high and low-frequency physical processes, such as tides, sea surface elevation, and river discharge, the latter being related to longitudinal baroclinic salinity gradient (Costa et al. 2020). Composed of four main estuarine channels (São Vicente, Piaçaguera, Bertioga and Porto de Santos), the SES is of great importance in large-scale activities, especially industries in Cubatão and the Santos' Harbour (Figure 1). The Santos Bay has five artificial channels responsible for leading diffuse rainfall from the city into the beaches, which are regulated by floodgates. They are kept closed during periods of low rainfall to prevent pollution due to the irregular discharge of sewage (da Silva Ferreira et al. 2021). However, such gates are opened in periods of significant rainfall, making the dispersion and transport of pollutants to Santos Bay an important factor.

The SES connects to the Inner Continental Shelf (ICS), where currents and sea surface height (SSH), are controlled by density gradients, tides and wind shear stress (Dottori & Castro 2009, Dottori & Castro 2018). Density gradients are caused by the discharge of continental waters which, when encountering waters from the shelf, generate geostrophic currents parallel to the coast (Costa et al. 2020). Wind shear presents the highest variability in driving currents and surface elevation. Prevailing easterly and northeasterly winds, intensified in summer, are the main pattern in this region, transporting surface waters offshore, and reducing the SSH (Dottori & Castro 2009). During the passage of frontal system events, winds transport waters towards the coast, contributing to increasing the SSH (Stech & Lorenzzetti 1992).

The M2 tidal harmonic is the most energetically significant (Dottori & Castro 2018). However, the tides are one order of magnitude lower than the perpendicular currents generated by the combination of wind shear stress and the density gradient (Costa et al. 2020).

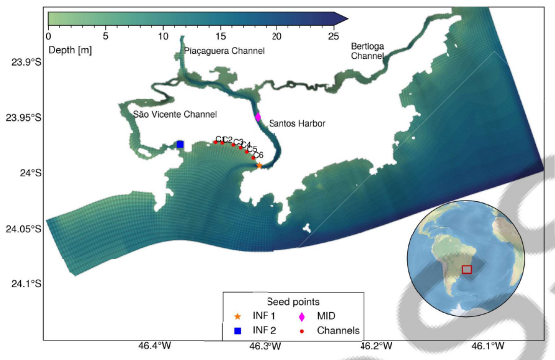

Figure 1. Santos Estuarine System bathymetry with its geographic location on the Brazilian coast (red square at the lower right globe), and the locations of seeding locations at the two stages of the experiments by coloured markers. The red circles represent the locations of the drainage channels, labelled with the respective number n (Cn).

Numerical Models

The Eulerian ECOM Model

The current velocity results simulated with the Estuarine and Coastal Ocean Model (ECOM) serve as an Eulerian basis for the OpenDrift Lagrangian framework. The ECOM – coastal and estuarine three-dimensional version of the Princeton Ocean Model (POM) (Blumberg & Mellor 1987) – simulates the conservative variables (temperature, pressure and salinity), currents and sea level through the solution of the momentum and continuity equations in an Arakawa C-grid in vertical sigma coordinates. Analytically, the ECOM employs the hydrostatic and the Boussinesq approximations, considering the density field perturbations with the vertical momentum component. Thus, there are prognostic variables such as the zonal, meridional and vertical components of velocity, temperature, salinity and elevation of the free sea surface through the Navier-Stokes momentum equations, continuity, and conservation of temperature and salinity, in sigma vertical coordinates (terrain following) (Blumberg &

Mellor 1987).

The SES curvilinear grid comprises the four main estuarine channels and Santos Bay, as well as the adjacent portion of ICS (Figure 1). It has 322 cells in the parallel direction by 132 cells in the perpendicular direction to the coastline in Santos Bay. Curvilinear grid lines are drawn to create an orthogonal grid with a low aspect ratio and relatively high horizontal resolution within estuarine channels. The average resolution is 144.5 m, ranging from 26.7 m at the São Vicente and Bertioga to 444.5 m at the southwest portion of the domain. Along the Santos Harbour, the horizontal resolution is approximately 100 m (Costa et al. 2020).

The simulations carried out in this study used the operational PreAMar system (Costa et al. 2020), developed to provide daily updated 72-hour forecasts of sea surface elevation and currents in the SES, forced by winds, tides and fluvial discharge (Costa et al. 2020). PreAMar presents its forecast based on seven tidal components (M2, S2, O1, K2, N2 and Q1) with phase distribution along the edge. The initial thermohaline conditions are from climatology (22.3°C, 30.4 PSU), and the thermohaline boundary conditions come from a regional domain over the SBB, as well as the sea and tidal free surface elevation boundary conditions. River discharge is variable through space with 13 freshwater discharge points, also varying through the seasons. Such Eulerian results were validated for the region and period covered by the simulations of the present study. (Costa et al. 2020).

The WaveWatchIII Wave Model

Significant wave height, Stokes drift and average wave period results were generated by the WaveWatch III wave model (ST6 formulation), which is a third-generation model developed at NOAA/NCEP based on Wave Modelling (WAM) (Komen 1994).

The WaveWatchIII equations include refraction and deformation of the wave field due to temporal and spatial variations in mean water depth, and mean current (e.g: tides, storm surges.). Wave propagation is considered linear, and relevant nonlinear effects, such as resonant interactions, are included in the source terms (Cavaleri et al. 2007).

The wave simulations consist of nesting two grids (global and South Atlantic grid), which provide the wave spectrum for an unstructured grid over the continental shelf off the state of São Paulo through its boundary conditions. The global and spatial grid resolution is respectively 2° followed by a 0.5° regional grid covering the São Paulo coast (27°S-22°S, extending to 200m depth), constrained at the edges by the directional wave spectrum generated through the nested simulation. Finally, this São Paulo coast unstructured grid is interpolated to match the high-resolution PreAmar grid within the Santos Estuarine System (SES).

The OpenDrift Lagrangian model

OpenDrift is an open-source framework based on the Python programming language, highly generic and modular for numerical Lagrangian drift modelling (Dagestad et al. 2018), in continuous development, through which recent studies investigated connections of biogeochemical processes in the South Brazil Bight (Mendes et al. 2022), and bacterial dispersion at Cananéia-Iguape Estuarine Complex (Birocchi et al. 2025). This framework is an offline model for computing Lagrangian drift, which is computationally economic when compared to an online model, in which the drift is computed along with the hydrodynamic fields in the Eulerian model.

The OceanDrift module – on which the PlasticDrift used here is based – is the fundamental module for passive particle drifting – particles that quickly adjust their velocities to the velocity field and do not affect the flow properties, thus satisfying the equations of the movement (Prants 2014). This module includes Stokes drift forcings and wind drag, among other easily enabled configurations (Dagestad & Röhrs 2019). In PlasticDrift, particles with sizes between 2 mm and 5 mm, are subjected to three-dimensional transport by currents, surface Stokes drift due to gravity waves, and wind drag. The vertical movement consists of buoyancy and mixing by oceanic turbulence, in which a random scheme of diffusivity in vortices depends on the wind (Strand et al. 2021).

The fourth-order Runge-Kutta scheme was used to integrate over a specific time interval and result in the position of the drifter in each time step, which duration was set as 60 seconds, through bidimensional nearest neighbour interpolation (Dagestad et al. 2018). Such a scheme assumes that a

particle is passive in a three-dimensional flow (Edwards et al. 2006). The integrated first-order partial differential equation with initial value condition (Ličer et al. 2020) is then solved to incorporate the Eulerian current, wind drag deviations (Callies et al. 2017), and the Stokes drift.

Experiments

To assess the annual export of microplastics from the SES to SBB, the dispersion of particles was simulated using OpenDrift for two subsequent years (2019 and 2020), with inert particles that do not interact with the temperature and salinity of the environment.

We chose 8 seeding locations in the SES domain (Figure 1). Six points are located near the artificial channels (C1 - C6) and two are arbitrary points (INF1 and INF2), chosen based on the surface and subsurface sources of solid waste in a Bay, such as factories, large urban centres, and junction flows (Kaandorp et al. 2021, Balthazar-Silva et al. 2020). For each seeding point, neutral buoyancy particles were released every hour throughout the whole 2 years of simulations.

Henceforward, beaching refers to the permanent retention of particles upon contact with coastal land (dry shoreline). Stranding is defined as beaching or the seabed contact without resuspension. So, there is no longer movement of the particles when they contact both the dry cells and the bottom of a wet cell

The artificial channels are opened during periods of intense rainfall to avoid urban flooding; however, the information about the opening of these channels is not available for public access, so we infer their opening based on the prediction regime of interest. For that, we used daily accumulated precipitation time series provided by the public administration of Santos for 2019 and 2020 (Figure 2), defining here hypothetical openings on the day and the following day of floodgates for a threshold of 2 standard deviations above the average rainfall.

High variability in marine litter abundance, including tidal swings, is especially evident in estuarine environments (Bettim et al. 2021). Monitoring a frequency comparable to spring and neap tidal cycles provides the necessary information to better understand the influence of meteorological and oceanographic conditions on the amount and type of debris on different coastlines (Moreira et al. 2016). Therefore, to quantify the vulnerability to contamination by microplastics in the SES in events of sea surface extreme elevation, the years 2019 and 2020 were simulated independently in OpenDrift in periods of 72 hours, to resolve half of a cycle of neap and spring tides.

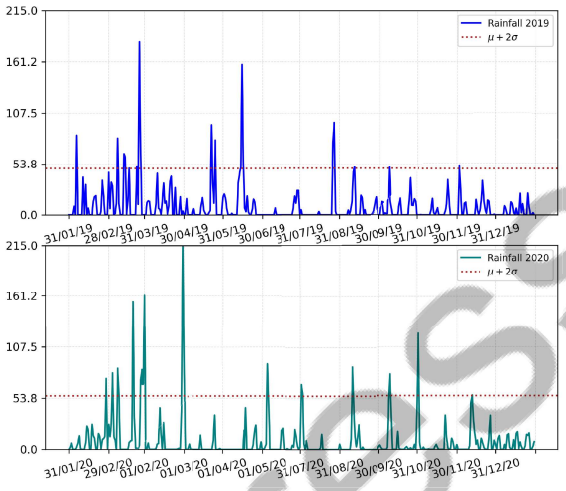

Figure 2. Rainfall [mm] at Santos City to 2019 (top) and 2020 (bottom). The red horizontal line indicates 2 standard deviations (σ) from the temporal average (μ).

We defined three categories of sea surface elevation based on statistical thresholds applied to the sea surface height (η) from the mean (μ) and the standard deviation from the mean (σ): (i) Extreme elevation, when the sea surface height exceeded two standard deviations above the mean ($\eta > \mu + 2\sigma$); (ii) Extreme decline, when it fell below two standard deviations from the mean ($\eta < \mu - 2\sigma$); and (iii) Normal elevation, when it remained within two standard deviations of the mean ($\mu - 2\sigma \leq \eta \leq \mu + 2\sigma$).

At each location (INF1, INF2, MID, and artificial channels C1–C6; see Figure 1), we released 42 neutrally buoyant particles per hour. These releases occurred every 72 hours over the course of a year. Particles were seeded at depths between 0 and 5 m to ensure accurate representation of both surface dispersion and subsurface transport dynamics, following the methodology of (Hardesty et al. 2017).

Analysis

The particle amount per unit area (km²) was calculated separately for 2019 and 2020 to estimate the annual export of microplastics to the continental shelf.

To quantify contamination, probability maps were generated to illustrate the likelihood of particles making contact with land, highlighting the regions within the Santos estuary and bay that are most prone to microplastic accumulation (Saçu et al. 2021).

The three-dimensional contact probability (P) is given by:

$$P(x, y, t) = \frac{1}{s} \sum_{\eta=1}^{S} \sum_{\tau=0}^{T} \frac{C(x, y, t)_{\eta,\tau}}{N_{\eta,\tau}} \qquad (1)$$

where $C(x, y, t)$ is the number of particles' contacts in a grid cell centred on x and y at a given time t, which varies between 0h and the total time of the simulation. N is the total number of simulated particles in time t, and S is the number of simulations at a given elevation configuration (η) through period (τ). Naturally, P ranges from 0 to 1 (Saçu et al. 2021). Through this probability, the temporal variation of the spatial movement of microplastics is evaluated.

The detection of accumulation hotspots was based on identifying regions where the probability of contact exceeded 5% , considering all particles released into the system. Each sea surface elevation condition was analysed separately, and the probability was evaluated at three-times intervals: 24, 48, and 72 hours.

For each 72 hours under a given elevation condition, the contact probability was calculated and then normalised by the total number of 72-hour periods corresponding to that specific elevation condition.

Dispersion validation and caveats

The main caveat of this work lies in the absence of *in situ* data for validation during the simulated periods. Nevertheless, by employing an Eulerian model that has been previously validated for this region and period, we compared the results of our simulations with the particle dispersal areas reported by Gorman et al (2020). Their study used a simplified Lagrangian approach, coupled with a coarser Eulerian model configured with a horizontal resolution fixed at 1 km and run for the year 2008.

The seeding points used in the present study were based on those of Gorman et al. (2020), with further adaptations based on Kaandorp et al. (2021). While the particle release locations are not identical, they are conceptually consistent. Given that the Eulerian model employed here has been validated and is capable of capturing the dominant and recurrent physical processes operating during the years 2019 and 2020 (Costa et al. 2020), we argue that the resulting dispersal areas can be reasonably compared with those from the earlier study.

The monthly-averaged dispersal patterns obtained here (presented in the next section in area values and percentual particle amount) are, in both percentual extent and spatial distribution (footprint), qualitatively similar to those presented by Gorman et al. (2020). Specially the seeded particles at INF1, INF2 and the artificial channels that match the beach region at Gorman et al. (2020), that spanned from around 70 km² -80 km² for INF1 and INF2, and near 20 km² for each channel.

We acknowledge that comparing results from two different modelling studies — rather than directly validating against observational data — is not ideal. However, in the absence of microplastic observational data for the specific years simulated and at matching spatial resolutions, this constitutes a form of indirect validation currently feasible, once Gorman et al. (2020) made *in situ* sampling at the Santos' beaches for 2008. The reader is refered to Gorman et al. (2020) for further details about MP footprint.

RESULTS

Natural Sources of Contamination

Figure 3 shows the time evolution of the particles released in INF1 and INF2, for 2019 and 2020, and the time that the particles are stranded at a dry cell (stranding time henceforward).

In 2019, the particle accumulation and exportation presented inverse patterns between INF1 and INF2 (Figure 3). For the INF1 (INF2) releasing point, particles presented an accumulation (exportation)

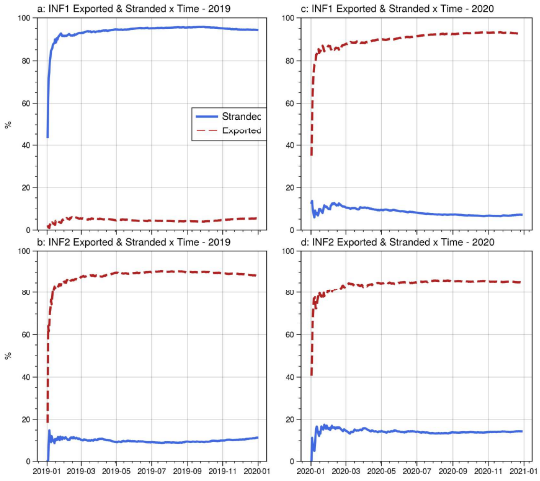

Figure 3. Cumulative export and stranding percentage by time for particles released in 2019 and 2020 in INF1 (a,c) and INF2 (b,d)

within the SES. Particularly for the INF1 location, this pattern affects directly the rate of particle accumulation, resulting in 94.6% particles stranded and only 5.4% exported to the SBB. Particles from INF1 reached an area of 70.37 km², while INF2 reached a much larger area of 130.48 km², due to the fast stranding of particles released in INF1, in the channel between Santos and Guarujá.

The 2020 scenario exhibited a similar pattern of stranding and exportation between seeding points INF1 and INF2. Throughout the analysis, particles were more frequently exported than stranded within the system (Figure 3c and d).

As in 2019, the export-to-stranding ratio influenced the dispersion area. However, unlike the previous year, the difference in coverage area between the two seeding points was approximately 30%. While INF1 covered an area of 88.65 km², INF2 reached a larger area of 122.78 km². Thus, the exportation rates between the seeding points in 2020 were similar: 92.6% for INF1 and 85.3% for INF2.

Artificial Sources of Contamination

Figure 4 illustrates the inverse relationship between particle export from the SES artificial channels and stranding along the coast or bay floor. Higher export rates corresponded to lower stranding rates. The

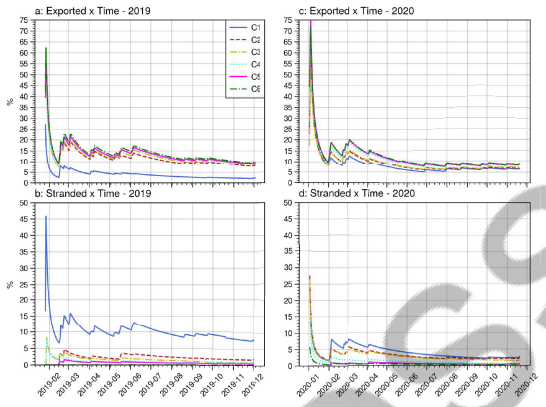

Figure 4. Cumulative percentage export (a,c) by time and stranding (b,d) by time for particles released in the artificial channels of Santos in 2019 and 2020.

logarithmic pattern shows periodic spikes coinciding with particle release events, indicating that both export and stranding occur shortly after seeding. Notably, channel C1 exhibited significantly different behaviour compared to the other channels (C2–C6), with over 0.56% fewer particles exported and 0.67% more particles stranded.

For the artificial channels, the percentage of exported particles increased from 2.3% at C1 to 10.1% at C6. Conversely, the total percentage of stranded particles followed an opposite trend, with the highest stranding occurring at C1 (7.85%) and the lowest at C6 (0.053%). This indicates a reduction in beach stranding as the channels transition from Santos toward Guarujá.

Additionally, in 2019, particles released at INF1 exhibited a significantly higher export rate, with nearly total stranding. The total affected area also decreased along the channels, from 34.062 km² at C1 to the smallest area of 17.121 km² at C6.

In 2020, similar to 2019, the total export increased progressively from C1 to C6, although the increment between C5 and C6 was smaller, only 0.13%. The total stranding also decreased progressively from C1 to C6, but with a smaller decline between the channels compared to 2019. This suggests that, as with exports, stranding was also lower in 2020, allowing particles to remain active in the system for a longer period.

The total dispersion areas were larger in 2020 than in 2019 due to the earlier opening of the flood-

gates—on the second day of 2020 compared to the second week of 2019. This earlier opening allowed more time for particle dispersion and exposed them to stronger currents, increasing the dispersion potential. However, unlike in 2019, the difference in export and stranding between C1 and the other artificial channels was much smaller in 2020. The difference between C1 and C2 was less than 100 stranded particles, as well as for those exported.

In summary, 17.8% of the particles released in 2019 were exported, compared to 28.12% in 2020. Meanwhile, the proportion of stranded particles decreased from 14.8% in 2019 to 3.7% in 2020 (not shown). These values further highlight that the exportation suppresses the stranding, and also indicate that most of the particles (67.4% in 2019 and 68.18% in 2020) keep active in the water column.

Tidal dynamics influence on microplastic retention

To understand the microplastic accumulation under different elevation scenarios, we computed the probability (%) of stranding. Only probabilities higher than 5% within all 72-hour periods were used, computing the total particles considering all seeding points. Therefore, this analysis gives an understanding of which sea surface elevation conditions the SES accumulates more marine litter.

Figure 5 presents the number of events in which the probability (%) of contact exceeded 5% over time within all 72-hour periods, considering the total amount of particles from all launch points. These results demonstrate that the system retains microplastics and increases contamination along the coast.

Under extreme subsidence conditions of sea surface elevation, the number of contact events with the shore was the lowest, both in terms of the number of affected points and the number of particles, regardless of the tidal phase. Thus, lower extreme elevations not only reduce particle accumulation along the coast but also enhance exportation and prolong the retention of microplastics within the water column of the bay.

During neap tide, a higher sea surface elevation led to an increased number of contacts with the mainland and more events where the probability of contact exceeded 5%. During spring tides, the greatest number of events with a contact probability above 5%, as well as a higher concentration of contaminated points (particularly in the interior of the Santos Channel and the São Vicente mouth), occurred under normal sea surface elevation conditions. Additionally, for all elevation conditions, the total number of contact events exceeding 5% probability was higher during spring tides.

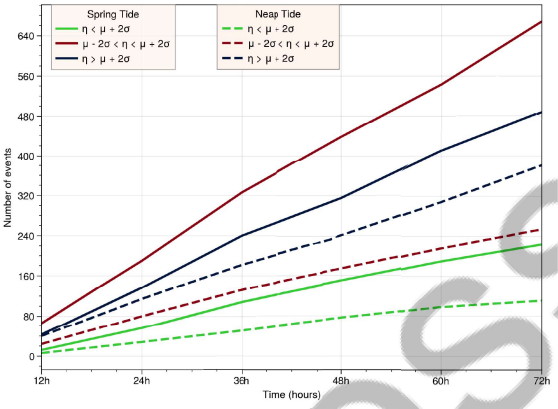

Figure 5. Number of events with a probability greater than 5% of contact with a dry cell over the time in the averaged 72h periods for 2019 and 2020 for all particles released in INF1, INF2, MID and the artificial channels (C1 - C6) according to sea surface height condition (η), mean (μ) and standard deviation (σ).

Thus, during spring tides, the highest contamination probability occurs under normal sea surface elevation conditions, whereas during neap tides, it is associated with extreme elevations. However, extreme subsidence consistently resulted in the lowest contamination levels across all surface elevation conditions.

To assess the likelihood of contamination, the three-dimensional probabilities of contact after 72 hours of simulation are presented for all seeding points with potential contamination in Santos Bay. These probabilities are expressed as percentages for each sea surface elevation condition. Additionally, the regions associated with a contact probability greater than 5% are highlighted.

Figure 6 illustrates these probabilities for neap and spring tides. Similarly, Figure 7 presents the corresponding analyses for the year 2020.

In 2020, particle dispersion extended to the outermost regions of the Southeastern Shelf (SES),

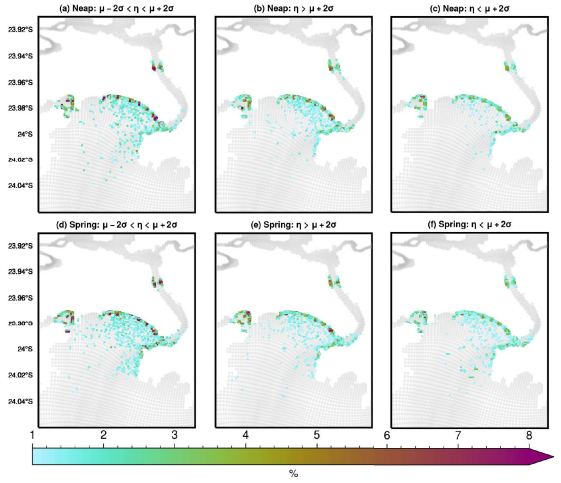

Figure 6. Probability of three-dimensional contactin SES during neap tide (a,b,c) and spring tide (d,e,f), after 72h of particles released in MID, INF1, IN2 and in channels C1 to C6 in 2019 between 0 and -5 m for $\mu - 2\sigma < \eta < \mu + 2\sigma$ (a,d), $\eta > \mu + 2\sigma$ (b,e), and $\eta < \mu + 2\sigma$ (d,f). According to sea surface height condition (η), mean (μ) and standard deviation (σ).

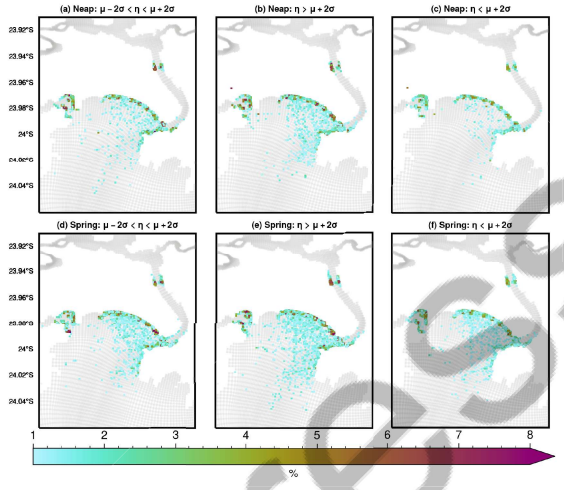

Figure 7. Probability of three-dimensional contact in SES during neap tide (a,b,c) and spring tide (d,e,f), after 72h of particles released in MID, INF1, IN2 and in channels C1 to C6 in 2020 between 0 and -5 m for $\mu - 2\sigma < \eta < \mu + 2\sigma$ (a,d), $\eta > \mu + 2\sigma$ (b,e), and $\eta < \mu + 2\sigma$ (d,f). According to sea surface height condition (η), mean (μ) and standard deviation (σ).

reaching areas near Guarujá. However, no contact probabilities exceeding 5% were observed beyond the channel exit between Santos and Guarujá or within Santos Bay (Figure 6).

Apart from the regions influenced by particles released at the MID point and the channel entrances near INF1 and INF2, no significant contact probability was detected within the SES or in the direction of Bertioga for any of the years studied.

For the 72-hour periods, the largest accumulations of particles, in both 2019 and 2020, during neap and spring tides – occurred along the coast (Figures 6 and 7). Contact probabilities greater than 5% were observed only on the beaches of Santos Bay, at the mouths of the Santos and São Vicente channels, and near the seeding points in the middle estuary. Contact events increased during each 12-hour period, with the lines representing the number of events with a contact probability greater than 5% becoming steeper toward the end of the period 5.

The lowest number of hotspots is observed under extreme subsidence conditions (Figures 9 a and 9 b). The highest number of hotspots occurs under extreme elevation conditions (Figures 8 b and 9 b), although it is only slightly higher than under normal elevation conditions during neap tide (Figure 8 c).

A greater number of hotspots is observed with the highest elevations, particularly in the middle portion of the channel between Santos and Guarujá, with an increase extending toward Guarujá and into the channel between Guarujá and Santos. Between the artificial channel C1 and the mouth of the São Vicente channel, no accumulation hotspots were detected. However, in the latter, there is a noticeable increase in the number of points more susceptible to microplastic contamination as surface elevation rises. The entire shore of Santos Bay, between the artificial channels, presents accumulation hotspots for microplastics under any sea surface elevation condition (η) (Figures 8 and 9).

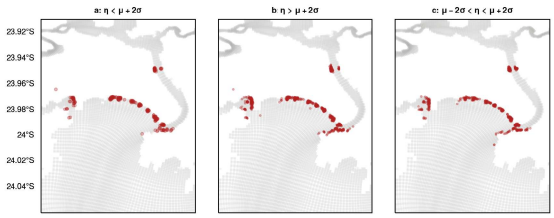

Figure 8. Hotspots (location with contact probability higher than 5 %) of microplastic accumulation in the SES during neap tide for $\eta < \mu + 2\sigma$ (a), $\eta > \mu + 2\sigma$ (b) and $\mu - 2\sigma < \eta < \mu + 2\sigma$ (c).

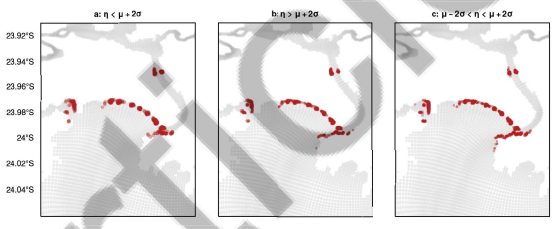

Figure 9. Hotspots (location with contact probability higher than 5 %) of microplastic accumulation in the SES during spring tide for $\eta < \mu + 2\sigma$ (a), $\eta > \mu + 2\sigma$ (b) and $\mu - 2\sigma < \eta < \mu + 2\sigma$ (c).

DISCUSSION

The largest dispersion in Santos Bay occurs when particles are seeded at the mouth of the São Vicente channel (Figures 6 and 7). These particles have the potential to reach the entire Bay of Santos and São Vicente, but with limited inland dispersion. This dispersion is primarily influenced by the tidal cycle, with exportation during ebb tide and accumulation during flood tide (Malli et al. 2022).

C6 is the closest station to the Porto Channel and, consequently, to the INF1 release point. This proximity resulted in contrasting outcomes between 2019 and 2020, with greater particle accumulation observed in 2019 and higher export in 2020. However, due to the dispersion patterns and the combined effects of particle export and stranding from INF2 and the artificial channels, the overall export of particles from the mouth of the Porto Channel to the South Brazil Bight (SBB) was more pronounced.

The preferential southwestward flow in the inner region of the SBB under high-pressure atmospheric synoptic conditions (Dottori & Castro 2009) enhances the export of microplastics from sources along this direction. This effect is further amplified by increased river discharge associated with the Porto channel, driven by deeper waters due to dredging activities and the connection between the Piaçaguera and Bertioga channels (Figure 1) (Pinheiro et al. 2021). Additionally, surface Stokes drift dynamics linked to the wave climate (Stein & Siegle 2019, Dagestad & Röhrs 2019), cold front incursions (Stech & Lorenzzetti 1992), and buoyancy advection from fresher waters toward the Equator contribute to the annual-scale dispersion of particles toward Guarujá and Bertioga. This combination of forces is also thought to be responsible for the drift of the exported particles from SES to the SBB towards the Equator, until they meet more complex dynamics. However, further study is needed for that conclusion.

The weakening of the tidal amplitude relative to river flow during neap tides intensifies ebb currents (Seiler et al. 2020). As a result, particles released at INF1 and within the artificial channels near the São Vicente channel exhibit a greater potential for dispersion and export, driven by stronger ebb currents at these locations compared to the Harbour channel (Figure 5).

The exportation results show that the SES has a greater annual potential for exporting microplastics to SBB than retention, while the hydrodynamic and differences associated with the Lagrangian model (Dagestad & Röhrs 2019) that made 2020 export more. The probability of contact demonstrated that in the SES, there is a greater accumulation of microplastics on the coast with increasing sea surface elevation, corroborating other studies (Gorman et al. 2020, Vermeiren et al. 2016, da Silva Ferreira et al. 2021).

The spring tide redistributes free particles in the water column that have remained since the neap tide (Malli et al. 2022). That is, during neap tide, the greater the elevation of the free surface, the greater the accumulation of particles on the shore. During the spring tide, however, the highest flood and ebb velocities redistribute the particles that remained active in the water column (Figure 5). During spring tide, favourable hydrodynamic conditions accumulate the remaining particles, from the previous neap tides on the coast, both under normal and extreme elevations.

Our results indicate an increase in contact points along the coast, leading to intensified beaching of particles near the port channel, particularly during spring tides in both 2019 and 2020. This pattern is primarily due to the lower ebb tide velocity compared to the flood tide in this region (Seiler et al. 2020).

The combination of ebb and flood tide variations, the limited area available for dispersion (Piehl et al. 2020), and the considerable depth relative to the narrow width of the channel forces surface and subsurface particles to run aground before they can reach lower-energy zones and disperse over a longer period (Röhrs et al. 2014). As a result, a higher frequency of events with contact probabilities exceeding 5% occurred during normal elevation phases of the spring tide.

In summary, the flood tide during spring promotes particle accumulation, while the regional ebb tide under normal elevation conditions is insufficient to remove them, leading to prolonged retention. However, during extreme elevations in spring tide, when astronomical forcing surpasses meteorological influences, the ebb tide becomes strong

enough to resuspend particles into the water column, preventing prolonged contact with the coast.

Regarding accumulation and the areas most susceptible to microplastic pollution in the Santos Estuarine System (SES), our results indicate that over short periods, comparable to a few tidal cycles, particles tend to accumulate and run aground near their release points, regardless of whether it is a spring or neap tide.

However, in annual simulations, accumulation becomes more extensive, spreading along the entire coast of Santos and São Vicente Bay, although concentrations remain higher near the sources. This pattern suggests that, similar to what was observed in Praia da Enseada do Guarujá (da Silva Ferreira et al. 2021), plastic accumulation in the SES is influenced by both proximity to the source and the morphological characteristics of the region. More importantly, the frequency of extreme elevation events plays a crucial role in determining the overall distribution and retention of microplastics.

SUMMARY

This study brings to SES the coupling between an Eulerian model, a spectral wave model and a Lagrangian model in offline mode. Such an approach is increasingly applied to studies of world ocean pollution, optimizing simulation time and error propagation of hydrodynamic fields drifting from floating microplastics neutral to quantify the potential for export, accumulation and dispersion of this growing form of pollution, identifying the regions most susceptible to contamination under different conditions of elevation of the sea surface.

Annually, through the density gradients and quantification of particles that leave the numerical grid of the SES and those that become attached to the dry cells, the SES has a greater potential for exporting microplastics to SBB (23% of the total released) than accumulation (8.9% of the total released). Most of the microplastics released annually in the SES (68.1%), however, remain active in the water column of the middle estuary and Santos Bay.

The hydrodynamic configuration of the system, characterised by a preferential southwestward flow, Stokes drift pushing waves toward the coast, hydrodynamic inversions due to cold front intrusions, and buoyancy-driven advection toward the northeast, collectively influence the movement of neutrally buoyant particles. These processes maintain particle activity within the Bay of Santos and the channels of Porto and São Vicente.

Thus, the SES exhibits a hydrodynamic regime that favours the sustained suspension of seeded particles in the water column, preventing their rapid deposition and prolonging their residence time in the system.

Extreme sea surface subelevation, defined as values below two standard deviations from the mean, reduces particle accumulation along the coast and enhances dispersion throughout Santos Bay, regardless of whether it occurs during spring or neap tides.

Conversely, sea surface elevations exceeding two standard deviations from the mean promote greater particle accumulation along the coast and reduce dispersion within Santos Bay. This effect is particularly pronounced toward the south due to hydrodynamic inversions associated with such extreme elevation conditions.

The spring tide plays a crucial role in transporting particles toward the coast that were not advected to the South Brazil Bight (SBB) during the neap tide. This transport pathway highlights the vulnerability of the Santos Estuarine System (SES) to microplastic contamination, particularly under extreme sea surface elevation events such as storm surges.

The areas most susceptible to microplastic contamination are those closest to the primary sources of microplastics, as well as regions influenced by channel curvature, width, and ebb tide velocity, which determines the efficiency of particle export from the estuary.

Despite variations in sea surface elevation, the SES remains an effective exporter of microplastics to the SBB. However, within the SES itself, hydrodynamic processes were not sufficient, even in annual simulations, to transport microplastics to locations further north of Guarujá. A three-dimensional analysis of contact probabilities further indicated that microplastic particles did not significantly enter the estuarine channels, as they tended to quickly run aground along the channel sides or settle on the bottom.

Although this study provides valuable insights into microplastic transport within the SES, further research is needed to refine our understanding of their dispersion patterns. Future studies should investigate microplastic behaviour under various extreme conditions, such as atmospheric blocking events, which induce sea surface subelevation while reducing river discharge (Silva & Dottori 2021), or extreme precipitation scenarios. Additionally, simulations with expanded numerical domains are necessary to track the fate of microplastics after they reach the SBB, which was beyond the scope of this study.

AUTHOR CONTRIBUTION

A.D. : Conceptualisation; Formal analysis; Investigation; Writing – original draft; Writing – review & editing;

D.A.S. : Conceptualisation; Investigation; Writing – review,

D.K.S. : Investigation; Writing,

M.D. : Conceptualisation, Supervision; Resources; Project Administration; Funding Acquisition; Writing - Review.

DATA AVAILABILITY STATEMENT

The codes for both Lagrangian and Eulerian analysis are available by contacting the authors.

CONFLICTS OF INTEREST

The authors declare that they have no conflict of interest.

FUNDING

The authors would like to acknowledge and thank Petróleo Brasileiro S.A. (PETROBRAS) for their financial support, provided through the USP Foundation (FUSP), for the duration of this project from 2019 to 2022.

REFERENCES

BALTHAZAR-SILVA, D., TURRA, A., MOREIRA, F. T., CAMARGO, R. M., OLIVEIRA, A. L., BARBOSA, L. & GORMAI
fall and tidal cycle regulate seasonal inputs of microplastic pellets to sandy beaches, *Frontiers in Environmental Science* 8, 123.

BETTIM, M., KRELLING, A. P., DI DOMENICO, M., CORNWELL, T. O. & TURRA, A. 2021. Daily environmental variation influences temporal patterns of marine debris deposition along an estuarine outlet in southern brazil, *Marine Pollution Bulletin* 172, 112859.

BIROCCHI, P., DIALECTAQUIZ, A. & DOTTORI, M. 2025. Particle dispersion and sewage pollution in a subtropical estuary under climate change and extreme events, *Estuarine, Coastal and Shelf Science* 315, 109153.
URL: *https://www.sciencedirect.com/science/article/pii/S027*

BLUMBERG, A. F. & MELLOR, G. L. 1987. A description of a three-dimensional coastal ocean circulation model, *Three-dimensional coastal ocean models* 4, 1–16.

CALLIES, U., GROLL, N., HORSTMANN, J., KAPITZA, H., KLEIN, H., MASSMANN, S. & SCHWICHTENBERG, F. 2017. Surface drifters in the german bight: model validation considering windage and stokes drift, *Ocean Science* 13(5), 799–827.

CAVALERI, L., ALVES, J.-H., ARDHUIN, F., BABANIN, A., BANNER, M., BELIBASSAKIS, K., BENOIT, M., DONELAN, M., GROENEWEG, J., HERBERS, T. ET AL. 2007. Wave modelling–the state of the art, *Progress in oceanography* 75(4), 603–674.

COSTA, C. G., LEITE, J. R. B., CASTRO, B. M., BLUMBERG, A. F., GEORGAS, N., DOTTORI, M. & JORDI, A. 2020. An operational forecasting system for physical processes in the santos-sao vicente-bertioga estuarine system, southeast brazil, *Ocean Dynamics* 70, 257–271.

DA SILVA FERREIRA, A. T., SIEGLE, E., RIBEIRO, M. C. H., SANTOS, M. S. T. & GROHMANN, C. H. 2021. The dynamics of plastic pellets on sandy beaches: a new methodologi-

cal approach, *Marine Environmental Research* 163, 105219.

DAGESTAD, K.-F. & RÖHRS, J. 2019. Prediction of ocean surface trajectories using satellite derived vs. modeled ocean currents, *Remote sensing of environment* 223, 130–142.

DAGESTAD, K.-F., RÖHRS, J., BREIVIK, Ø. & ÅDLANDSVIK, B. 2018. Opendrift v1. 0: a generic framework for trajectory modelling, *Geoscientific Model Development* 11(4), 1405–1420.

DOTTORI, M. & CASTRO, B. M. 2009. The response of the sao paulo continental shelf, brazil, to synoptic winds, *Ocean dynamics* 59(4), 603–614.

DOTTORI, M. & CASTRO, B. M. 2018. The role of remote wind forcing in the subinertial current variability in the central and northern parts of the south brazil bight, *Ocean Dynamics* 68(6), 677–688.

EDWARDS, K., WERNER, F. & BLANTON, B. 2006. Comparison of observed and modeled drifter trajectories in coastal regions: an improvement through adjustments for observed drifter slip and errors in wind fields, *Journal of Atmospheric and Oceanic Technology* 23(11), 1614–1620.

EGGER, M., SULU-GAMBARI, F. & LEBRETON, L. 2020. First evidence of plastic fallout from the north pacific garbage patch, *Scientific reports* 10(1), 7495.

GOLDENBERG, S. B., LANDSEA, C. W., MESTAS-NUÑEZ, A. M. & GRAY, W. M. 2001. The recent increase in atlantic hurricane activity: Causes and implications, *Science* 293(5529), 474–479.

GORMAN, D., GUTIÉRREZ, A. R., TURRA, A., MANZANO, A. B., BALTHAZAR-SILVA, D., OLIVEIRA, N. R. & HARARI, J. 2020. Predicting the dispersal and accumulation of microplastic pellets within the estuarine and coastal waters of south-eastern brazil using integrated rainfall data and lagrangian particle tracking models, *Frontiers in Environmental Science* 8, 559405.

HANSEN, D. V. & RATTRAY, M. 1962. Classic article: Gravitational circulation in straits and estuaries, *Journal of Marine Research* 23 (1), 102–122.

HARDESTY, B. D., LAWSON, T., VAN DER VELDE, T., LANSDELL, M. & WILCOX, C. 2017. Estimating quantities and sources of marine debris at a continental scale, *Frontiers in Ecology and the Environment* 15(1), 18–25.

KAANDORP, M. L. A., LOBELLE, D., KEHL, C., DIJKSTRA, H. A. & VAN SEBILLE, E. 2023. Global mass of buoyant marine plastics dominated by large long-lived debris, *Nature Geoscience* 16(8), 689–694.
URL: *https://doi.org/10.1038/s41561-023-01216-0*

KAANDORP, M. L., YPMA, S. L., BOONSTRA, M., DIJKSTRA, H. A. & VAN SEBILLE, E. 2021. Using machine learning and beach cleanup data to explain litter quantities along the dutch north sea coast, *Ocean Science Discussions* 2021, 1–33.

KERSHAW, P., TURRA, A., GALGANI, F. ET AL. 2019. Guidelines for the monitoring and assessment of plastic litter and microplastics in the ocean.

KOMEN, G. 1994. Dynamics and modelling of ocean waves, *Dynamics of Atmosphere and Oceans* 25(4), 276.

KRELLING, A. P., SOUZA, M. M., WILLIAMS, A. T. & TURRA, A. 2017. Transboundary movement of marine litter in an estuarine gradient: evaluating sources and sinks using hydrodynamic modelling and ground truthing estimates, *Marine pollution bulletin* 119(1), 48–63.

LEBRETON, L. C., VAN DER ZWET, J., DAMSTEEG, J.-W., SLAT, B., ANDRADY, A. & REISSER, J. 2017. River plastic emissions to the world's oceans, *Nature communications* 8(1), 15611.

LIČER, M., ESTIVAL, S., REYES-SUAREZ, C., DEPONTE, D. & FETTICH, A. 2020. Lagrangian modelling of a person lost at sea during the adriatic scirocco storm of 29 october 2018, *Natural Hazards and Earth System Sciences* 20(8), 2335–2349.

MACLEOD, M., ARP, H. P. H., TEKMAN, M. B. & JAHNKE, A. 2021. The global threat from plastic pollution, *Science* 373(6550), 61–65.

MALLI, A., CORELLA-PUERTAS, E., HAJJAR, C. & BOULAY, A.-M. 2022. Transport mechanisms and fate of microplastics in estuarine compartments: a review, *Marine Pollution Bulletin* 177, 113553.

MARENGO, J., MULLER-KARGER, F., PELLING, M., REYNOLDS, C. J., MERRILL, S. B., NUNES, L. H., PATERSON, S., GRAY, A. J., LOCKMAN, J. T., KARTEZ, J., MOREIRA, F., GRECO, R., HARARI, J., SOUZA, C., ALVES, L., HOSOKAWA, E. & TABUCHI, E. 2017. An integrated framework to analyze local decision making and adaptation to sea level rise in coastal regions in selsey (uk), broward county (usa), and santos (brazil), *American journal of climate change* .

MENDES, C. B., CORTEZ, T., SANTOS, C. S. G., SOBRAL-SOUZA, T., SANTOS, A. D., SASAKI, D. K., SILVA, D. A., DOTTORI, M. & ANDRADE, S. C. S. 2022. Seascape genetics in a polychaete worm: Disentangling the roles of a biogeographic barrier and environmental factors, *Journal of Biogeography* 49(12), 2296–2308.

MOREIRA, F. T., PRANTONI, A. L., MARTINI, B., DE ABREU, M. A., STOIEV, S. B. & TURRA, A. 2016. Small-scale temporal and spatial variability in the abundance of plastic pellets on sandy beaches: methodological considerations for estimating the input of microplastics, *Marine Pollution Bulletin* 102(1), 114–121.

PIEHL, S., ATWOOD, E. C., BOCHOW, M., IMHOF, H. K., FRANKE, J., SIEGERT, F. & LAFORSCH, C. 2020. Can water constituents be used as proxy to map microplastic dispersal within transitional and coastal waters?, *Frontiers in Environmental Science* 8, 92.

PINHEIRO, L., AGOSTINI, V., LIMA, A., WARD, R. & PINHO, G. 2021. The fate of plastic litter within estuarine compartments: an overview of current knowledge for the transboundary issue to guide future assessments, *Environmental Pollution* 279, 116908.

POULAIN, M., MERCIER, M. J., BRACH, L., MARTIGNAC, M., ROUTABOUL, C., PEREZ, E., DESJEAN, M. C. & TER HALLE, A. 2018. Small microplastics as a main contributor to plastic mass balance in the north atlantic subtropical gyre, *Environmental science & technology* 53(3), 1157–1164.

PRANTS, S. 2014. Chaotic lagrangian transport and mixing in the ocean, *The European Physical Journal Special Topics* 223(13), 2723–2743.

RÖHRS, J., CHRISTENSEN, K. H., VIKEBØ, F., SUNDBY, S., SAETRA, Ø. & BROSTRÖM, G. 2014. Wave-induced transport and vertical mixing of pelagic eggs and larvae, *Limnology and oceanography* 59(4), 1213–1227.

SAÇU, Ş., ŞEN, O. & ERDIK, T. 2021. A stochastic assessment for oil contamination probability: A case study of the bosphorus, *Ocean Engineering* 231, 109064.

SEILER, L., FIGUEIRA, R. C. L., SCHETTINI, C. A. F. & SIEGLE, E. 2020. Three-dimensional hydrodynamic modeling of the santos-são vicente-bertioga estuarine system, brazil, *Regional Studies in Marine Science* 37, 101348.

SILVA, D. A. & DOTTORI, M. 2021. The atmospheric blocking influence over the south brazil bight during the 2013–2014 summer, *Regional Studies in Marine Science* 45, 101815.
URL: *https://www.sciencedirect.com/science/article/pii/S23*

STECH, J. L. & LORENZZETTI, J. A. 1992. The response of the south brazil bight to the passage of wintertime cold fronts, *Journal of Geophysical Research: Oceans* 97(C6), 9507–9520.

STEIN, L. P. & SIEGLE, E. 2019. Santos beach morphodynamics under high-energy conditions, *Revista Brasileira de Geomorfologia* 20(3).

STERL, M. F., DELANDMETER, P. & VAN SEBILLE, E. 2020. Influence of barotropic tidal currents on transport and accumulation of floating microplastics in the global open ocean, *Journal of Geophysical Research: Oceans* 125(2), e2019JC015583.

STRAND, K. O., HUSERBRÅTEN, M., DAGESTAD, K.-F., MAURITZEN, C., GRØSVIK, B. E., NOGUEIRA, L. A., MELSOM, A. & RÖHRS, J. 2021. Potential sources of marine plastic from survey beaches in the arctic and northeast atlantic, *Science of the Total Environment* 790, 148009.

VAN SEBILLE, E., ENGLAND, M. H. & FROYLAND, G. 2012. Origin, dynamics and evolution of ocean garbage patches from observed surface drifters, *Environmental Research Letters* 7(4), 044040.

VERMEIREN, P., MUÑOZ, C. C. & IKEJIMA, K. 2016. Sources and sinks of plastic debris in estuaries: a conceptual model integrating biological, physical and chemical distribution mechanisms, *Marine Pollution Bulletin* 113(1-2), 7–16.

This preprint was submitted under the following conditions:

- The authors declare that they are aware that they are solely responsible for the content of the preprint and that the deposit in SciELO Preprints does not mean any commitment on the part of SciELO, except its preservation and dissemination.
- The authors declare that the necessary Terms of Free and Informed Consent of participants or patients in the research were obtained and are described in the manuscript, when applicable.
- The authors declare that the preparation of the manuscript followed the ethical norms of scientific communication.
- The authors declare that the data, applications, and other content underlying the manuscript are referenced.
- The deposited manuscript is in PDF format.
- The authors declare that the research that originated the manuscript followed good ethical practices and that the necessary approvals from research ethics committees, when applicable, are described in the manuscript.
- The authors declare that once a manuscript is posted on the SciELO Preprints server, it can only be taken down on request to the SciELO Preprints server Editorial Secretariat, who will post a retraction notice in its place.
- The authors agree that the approved manuscript will be made available under a Creative Commons CC-BY license.
- The submitting author declares that the contributions of all authors and conflict of interest statement are included explicitly and in specific sections of the manuscript.
- The authors declare that the manuscript was not deposited and/or previously made available on another preprint server or published by a journal.
- If the manuscript is being reviewed or being prepared for publishing but not yet published by a journal, the authors declare that they have received authorization from the journal to make this deposit.
- The submitting author declares that all authors of the manuscript agree with the submission to SciELO Preprints.